Applied Mathematics & Information Sciences
An International Journal

http://dx.doi.org/10.18576/amis/180305

New Thresholding Function for Denoising and Deconvolution Discrete Doppler Wave

Maha M. Helmi

Department of Mathematics and Statistics, College of Science, Taif University, P.O. Box 11099, Taif 21944, Saudi Arabia

Received: 22 Nov. 2023, Revised: 18 Jan. 2024, Accepted: 19 Feb. 2024
Published online: 1 May 2024

Abstract: Speckle noise has a negative impact that results in information loss for images. As a result, this work has developed a new thresh function and began the study of the wave as a discrete. Then, estimate the underlying wave by removing the noise, blurring, and sharp features. The form of the universal threshold is carefully developed and is the key to the outstanding outcomes received in the extensive numerical simulations of wave and image denoising introduced here. A smooth wavelet basis is applied in this work, where each wavelet basis has N vanishing moments; more precisely, all coefficients of any polynomial of degree N or less will be exactly zero. A description of the wave using a new proposed method is investigated. The thresholding rule, whether hard or soft, is to threshold or shrink some wavelet coefficients towards zero. Comparing that method with another one, such as classical thresh resulting in kills, keeps the wavelet coefficients, and some wavelet coefficients are shrunk using the normal distribution. That method for the wavelet analysis is not suitable.

Keywords: Wave; Covariance matrix; wavelet; Frequency; De-noising, De-blur.

1 Introduction

In applied mathematics, wavelet, first present in seismology, received much research attention, see[1]. Wavelet transform approaches focus on obtaining a higher compression ratio without sacrificing image quality, and they now offer a promising approach to image compression. The wavelet generality and results benefit various applications, including signals and numerical analysis, [2], [3], [4]. Doppler waves are signals a medical machine generates, such as an automated external defibrillator. Most of the time, this machine is used to aid patients. Pulse wave Doppler (PW) employs the Doppler fundamental that moving objects change the characteristics of sound waves by sending short and fast sound pulses. In the mid-1800s, Christian Andreas Doppler observed that when a sound wave of a specific frequency hits a moving object, it will be reflected with a various frequency. This technique is called the Doppler effect. The principle was introduced in [5], who popularized the concept of vascular ultrasound imaging. At the end of the 20th century, transcranial Doppler (TCD) ultrasound in clinical practice for assessing cerebral hemodynamics opened a new generation in cerebral circulation monitoring introduced by [6]. Over the past few decades, ancient techniques have been used in heavy care components, surgical laboratories, invasive cardiology, and routine medical technique status; see [7], [8]. The advancement of Doppler ultrasound technology has proven to be an emergent tool in assessing various physiological dynamics, including heartbeat and respiration. The most known and commonly used technologies for hydrodynamic monitoring allow the measurement and acquisition of the two most common physical parameters: pressure and flow. These parameters are essential in describing the dynamics of blood flowing through the vessels. Other significant measurement parameters (distance, areas, and volumes) precisely correlated to “dynamics” correspond to medical imaging. Concurrently with the pressure and flow measurement methods, researchers described some complementary techniques to calculate different parameters directly related to hydrodynamics (i.e., pulse wave velocity, oxygen saturation, ballistocardiograph, cardiac contractility, cardiac wall motion, etc.) because their measuring and monitoring are quite familiar in additional hospital environments. However, their usage has improved with specialized advancements in medical instrumentation. The scanner can be provided for

* Corresponding author e-mail: m.hlmi@tu.edu.sa

continuous and pulse wave Doppler applications. One part is activated continuously during wave scanning, and the other obtains feedback. In contrast, during pulse wave scanning, a short burst or pulse activates a transducer component, and the same component obtains the return feedback. This information will only believe pulse wave scanning using both B-mode and Doppler methods. B-mode or grayscale images are used to locate the area or structure of interest for Doppler evaluation and serve as a background for the color representation of blood flow. Common terms associated with Doppler ultrasound are italicized for equine veterinarians and biologists on the principles using pulse wave Doppler imaging; see [9], [10]. To sample blood flow velocity at a specific location in the artery lumen, a combination of two-dimensional grayscale ultrasound to image arterial structures and pulse wave Doppler. A range of studies can be performed with the Doppler wave, using those waves by most patients with multilevel superficial femoral artery restenosis as an example. This makes it substantial in the evaluation of arteries and blood vessels. The anatomical location of the stenos is and the degree of stenosis can be estimated using continuous Doppler, Doppler waveforms, duplex imaging, and velocity changes in the circuit. Changes in the Doppler waveform are similar to those seen in continuous wave Doppler, but the speed can be estimated because the source of the signal sampling is known. The turbulent flow also leads to a spectral broadening of the Doppler signal; see [11], [12]. The article is organised as: Section 2 provides the problem, section 3 gives thresholding rules. In section 3 provides the procedure for choosing the parameters α_1 and α_2, Section 5 gives an extensive simulation. Section 6 provides an application to medical data. Section 7 gives conclusion.

2 Problem statement

Suppose the model of described wave is given by

$$y_i = \beta_i + \varepsilon_i \tag{1}$$

where y_i is set of the observation, β_i is the unknown parameters. This means that the true wave is corrupted by noise $\varepsilon_i \sim N(0, \sigma^2)$. For example, recording a voice with a background of wind. The second model is receiving waves with low frequency, the model can be written as

$$y_i = \sum_j Z_{ij}\beta_i + \varepsilon_i, \text{ if } i = 1,2,3,\ldots,n, \tag{2}$$

where $\sum_j Z_{ij}\beta_i$ is the true wave effects by transformation matrix and Z_{ij} is an element in the transform matrix. For example, a vocal tuner corrects the voice at the studio. However, the transform matrix is sometimes used to solve inverse problems. Figure 1 shows the plots of the transform matrix chosen as normal distribution and it takes the form

$$Z_{ij} = \exp\left(\frac{|i-j|}{\gamma}\right), i = j = 1,2,3,\ldots,n, \tag{3}$$

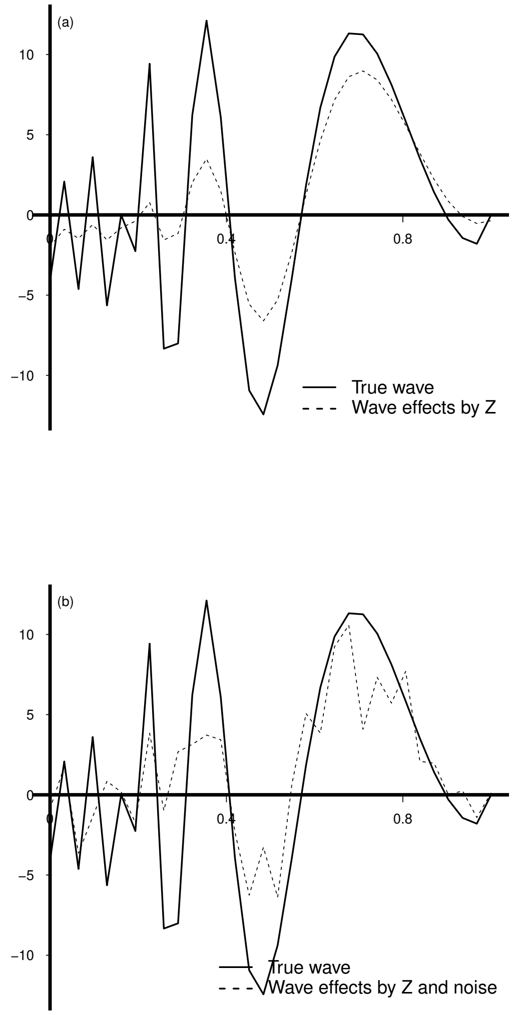

Fig. 1: Plots of the true wave (solid lines), the impact of a matrix transformation (dashed line) with $\gamma = 0.05$ in (3);(a) and the impact of the matrix transformation and noise (dashed line) with $\gamma = 0.05$ in (3) and normal independent noise equals 0.5; (b).

as γ increases the features of wave are vanish. The goal is to estimate β with small L_2 risk

$$R(\beta - \hat{\beta}) := \frac{1}{n}\sum_{i=1}^{n} E(\beta - \hat{\beta})^2. \tag{4}$$

Hence the second model can be explained the transformation matrix and noise effect the true wave. The main idea of the wavelet method is to write the signal as

$$h_s(x) = C_0\psi_{0,0}(x) + \sum_{j=0}^{s}\sum_{k=0}^{2^j-k} D_{j,k}\phi_{j,k}(x), \;\; x \in \mathbb{R}^j, \qquad (5)$$

where $C's$ are the average coefficients, and $C_0 =< \phi^0_{0,k}, y >= \sum_k \phi^0_{0,k} y_i$, while $D^j_{j,k} =< \psi^j_{j,k}, y >$ are the different coefficients, p is the power of the data such that $n = 2^s$, k is the location of the coefficient at level j, note that $k = 2^j - 1$. Hence, the non-parameters in (3) take the form

$$C_{j,k} = \frac{1}{n}\sum_{i=0}^{2^j-1} \phi_{j,k}(x_i)y_i, \;\; D_{j,k} = \frac{1}{n}\sum_{i=0}^{2^j-1} \psi_{j,k}(x_i)y_i, \qquad (6)$$

Figure 2 shows the impact of the transformation matrix, where the value of the parameter $\gamma = 0.05$ as $\gamma \to \infty$, the shape of the wave becomes flat;2(a). Also, the combination between matrix transformation and noise can be seen in 2(b). Moreover, $\psi_{j,k}$ is called the father wavelet, is given

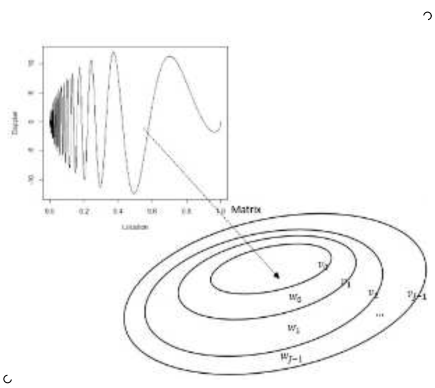

Fig. 2: Diagram showing the translation wavelet coefficients form data.

by

$$\phi_{j,k}(x) = \begin{cases} 2^{j/2}\phi(2^j x - k), & \text{if } j \in \mathbb{Z}, \;\; 0 \le k \le 2^J - 1, \\ 0, & \text{O.W}, \end{cases} \qquad (7)$$

and the mother wavelet is given as

$$\psi j,k(x) = \begin{cases} 2^{j/2}\psi(2^j x - k), & \text{if } j = j_0, j_0+1, \ldots, \log_2(n), \\ 0, & \text{O.W}, \end{cases} \qquad (8)$$

where n is the number of the data. In this article, the smooth wavelet basis is applied, where each wavelet basis has N vanishing moments, more precisely, all coefficients of any polynomial of degree N or less, will be exactly zero. Note that as the number of vanishing moments increases, the basis of the wavelet becomes smooth. The wavelet basis with 10 vanishing moments of extremal phase wavelet family, and then there are 20 possible filters, which are written as

$$H = \begin{bmatrix} 2.667006e-02 & 1.881768e-01 & 5.272012e-01 & 6.884590e-01 & 2.811723e-01 \\ -2.498464e-01 & -1.959463e-01 & 1.273693e-01 & 9.305736e-02 & -7.139415e-02 \\ -2.945754e-02 & 3.321267e-02 & 3.606554e-03 & -1.073318e-02 & 1.395352e-03 \\ 1.992405e-03 & -6.858567e-04 & -1.164669e-04 & 9.358867e-05 & -1.326420e-05 \end{bmatrix}.$$

Now, suppose that at level j, $v_j \in \mathbf{V}$ and $w_j \in \mathbf{W}$, then

$$\begin{aligned} v_j(x) &= \sum_k C_{j,k}\psi_{j,k}(x) \\ &= \sum_k C_{j-1,k}\psi_{j-1,k}(x) + \sum_k D_{j-1,k}\phi_{j-1,k}(x) \\ &= v_{j-1,k} + w_{j-1,k}, \end{aligned} \qquad (9)$$

where $C_{j-1,k} = \sum_k h_{k-2n}C_{j,k}$ and h is high-pass filter wave $D_{j-1,k} = \sum_k g_{k-2n}D_{j,k}$ and g is low-pass filter wave. Figure 2 shows a wave function introduced by Donoho, and Johnstone, (1994)–see [11] for more detail. The relationship between the average coefficients $C's$ and the difference wavelet coefficients $D'c$ and the location at each level. This means that $v_j = v_{j-1} \bigoplus w_{j-1}$, where $v_1 < v_2 < \cdots < v_{j-1}$, $w_1 < w_2 < \cdots < w_{j-1}$ and $\bigoplus_j w_j = L^2(\mathbb{R})$. Moreover, the level v_j contains two different coefficients, the first v_{j-1} which contains the scaling wavelet coefficients $C_{j-1,k}$ and the other is $w_{j-1,k}$ which contains the mother wavelet coefficients. If the haar wavelet basis is chosen then the 4×4 transformation matrix L is given by

$$L = \begin{bmatrix} \frac{1}{2} & \frac{1}{2} & \frac{1}{2} & \frac{1}{2} \\ \frac{1}{\sqrt{2}} & -\frac{1}{\sqrt{2}} & 0 & 0 \\ 0 & 0 & \frac{1}{\sqrt{2}} & -\frac{1}{\sqrt{2}} \\ \frac{1}{2} & -\frac{1}{2} & \frac{1}{2} & -\frac{1}{2} \end{bmatrix}_{4\times 4},$$

where the element in the matrix indicates to the low-pass filter and high-pass filter L. Hence, the first row in the matrix L gives the scaling wavelet coefficients at level 3 and the other rows give the mother wavelet coefficients at level $0, 1.$ and 2. For example, let $\mathbf{y} = \{3, 1, 4, 7\}$, then

$$Ly = \begin{bmatrix} \frac{1}{2} & \frac{1}{2} & \frac{1}{2} & \frac{1}{2} \\ \frac{1}{\sqrt{2}} & -\frac{1}{\sqrt{2}} & 0 & 0 \\ 0 & 0 & \frac{1}{\sqrt{2}} & -\frac{1}{\sqrt{2}} \\ \frac{1}{2} & -\frac{1}{2} & \frac{1}{2} & -\frac{1}{2} \end{bmatrix} \%*\% \begin{bmatrix} 3 \\ 1 \\ 4 \\ 7 \end{bmatrix} = \begin{bmatrix} 7.5 \\ 1.414214 \\ -2.121320 \\ -3.5 \end{bmatrix},$$

to invert the wavelet coefficients $\{7.5, 1.414214, -2.121320, -3.5\}$. In this example haar

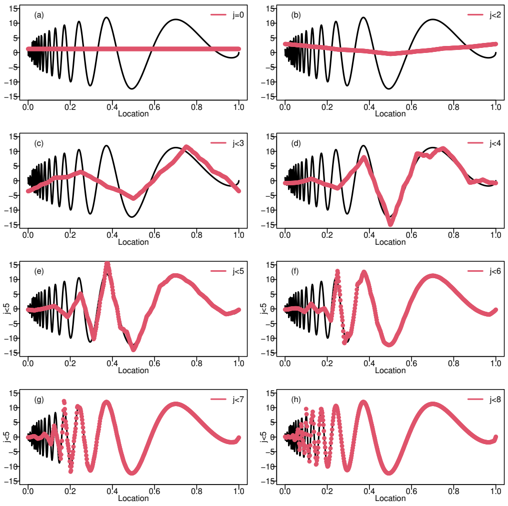

Fig. 3: Plots of cumulative approximations of Doppler wave, at $n = 512$ equally spaced points, at successive levels $s = \{0,1,2,3,4,5,6,7\}$, with the data shown as points.

basis is used, including the mother and the father wavelet are implemented to generate the low-pass and high-pass filters. Hence, $y = L^T Ly$, where $L^T L = I$. Figure 5 shows the plots of Doppler test function (black lines) and the function at each spaces are plots (red lines). For example, figure 5(a) shows the wavelet coefficients at level $j = 0$, where only father wavelet function is applied, while 5(b) shows the wavelet coefficients at level $j = 1$, where the father wavelet function at level $j = 0$ and the mother wavelet function at level $j = 1$ are applied. Hence, the reconstruction become more accurate as $j \to 2^{J-1}$ where $J = \log_2(n)$. Moreover, the wavelet coefficients at high level, such as $2^{j-1} - 1$, become closed and as number of data increases the number of wavelet increases and vice versa at low level. Finally, the wavelet topic is more complex and slightly difficult. It can not be covered without taking about decimated and non-decimated transformations. However, the decimated transformation is implicated, which can make this article easy to understand. For more knowledge, the easiest book can be read which is written by Nason–see [13], for more theoretical article, Vidakovic wrote a good book about wavelet and explained the basic idea–see [14], [15] and [16] who talked about the high and the low solution levels and showed how the narrow and the wide the wavelet coefficients are stretched out. For complex wavelet can be found in [17], they calculate the real and imagery wavelet coefficients and then treat the wavelet coefficients and invert the result. However, the imagery wavelet coefficients have a negligible effect.

3 Thresholding rules

There are several methods of thresholding were introduced in the past decades. The easy way to obtain shrinkage estimates of the true coefficients is to use thresholding rule [18]. The main idea of a thresholding rule is to threshold or shrink some wavelet coefficients towards zero, while the other kept. For example, Hard thresholding rule is the one of the classical rule which 'kill' or 'kept' some wavelet coefficients–see [19]. The function of the Hard thresholding for the first model in (1) can be written as

$$H_\alpha((Ly)_{j,k},\alpha) = \begin{cases} 0, & \text{if } |(Ly)_{j,k}| \le \alpha, \\ (Ly)_{j,k}, & \text{O.W}, \end{cases} \quad (10)$$

where $h(.)$ indicates to the Hard thresholding rule and Ly and then the wavelet coefficients are inverted $L^T h(Ly)$ and the parameter α indicates the threshold value. The result of Hard thresholding estimator is obtained by

$$\hat{\beta}_i = h_\alpha\left(\sum_j L_{ij} y_i, \alpha\right), \; j = 1,2,\ldots,n, \quad (11)$$

Also, the second thresholding rule is Soft thresholding which is competed the wavelet coefficients using the slope and the intercept. The Soft thresholding function for the first model in (1) can be written as

$$S_\alpha((Ly)_{j,k},\alpha) = \begin{cases} 0, & \text{if } |Ly| \le \alpha, \\ (Ly)_{j,k} + \alpha, & \text{if } (Ly)_{j,k} > \alpha, \\ (Ly)_{j,k} - \alpha, & \text{if } (Ly)_{j,k} < \alpha \end{cases} \quad (12)$$

where $S(.)$ indicates to the Soft thresholding rule. In this article, the new thersholding rule depends on two parameters α_1 and α_2 is proposed, and the function for the first model in (1) can be written as

$$M_{\alpha_1,\alpha_2}((Ly)_{j,k},\alpha_1,\alpha_2) \quad (13)$$
$$= \begin{cases} 0, & \text{if } |(Ly)_{j,k}| \le \alpha_1, \\ \sqrt{\frac{|\alpha_1-\alpha_2|}{\pi}} & \\ \times \exp\{-|\alpha_1-\alpha_2| \, ||(Ly)_{j,k}||_2^2\}, & \text{if } \alpha_1 < |(Ly)_{j,k}| < \alpha_2, \\ (Ly)_{j,k}, & \text{if } |(Ly)_{j,k}| \ge \alpha_2, \end{cases}$$

where $S(.)$ indicates to the proposed thresholding rule. The medial part in (13) can be explained as normal distribution. This thresholding rule kills, keeps the wavelet coefficients and some wavelet coefficients are shrunk using normal distribution. Note that

$$\lim_{\alpha_1 \to \alpha_2} M_{\alpha_1,\alpha_2}((Ly)_{j,k},\alpha_1,\alpha_2) = h_{\alpha_1}((Ly)_{j,k},\alpha_1), \quad (14)$$

while the function of rule takes normal distribution between the parameters α_1 and α_2. Figure 6 shows the plots of different thresholding rules. Note that all thersholding rules kill the wavelet coefficients around zero, in the interval $[-\alpha_1,\alpha_1]$. The new proposed and the

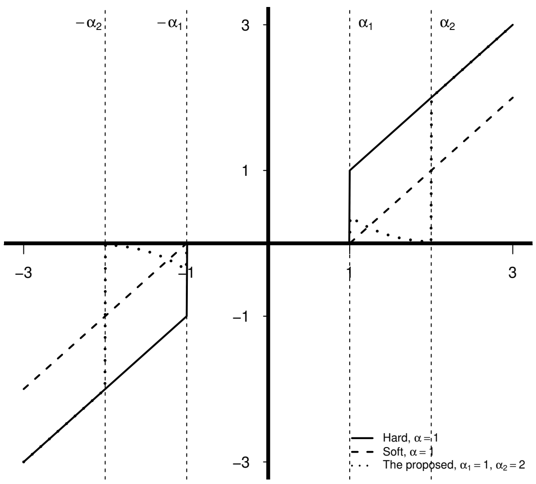

Fig. 4: Plots of thersholding rules Hard, Soft and the new threshold rule for different values of α_1 and α_2.

Hard thersholding rules keep the wavelet coefficients outside the intervals $[-\infty,-\alpha]$ and $[\alpha,\infty]$. The mean, variance and the risk of the proposed function, are given by

$$\text{Mean}_{\alpha_1,\alpha_2}((L\beta)_{j,k}) = \text{E}(M_{\alpha_1,\alpha_2}((Ly)_{j,k},\alpha_1,\alpha_2)) \quad (15)$$
$$\text{Var}_{\alpha_1,\alpha_2}((L\beta)_{j,k}) = \text{Var}(M_{\alpha_1,\alpha_2}((Ly)_{j,k},\alpha_1,\alpha_2)) \quad (16)$$
$$\text{R}_{\alpha_1,\alpha_2}((L\beta)_{j,k}) = \text{Var}(M_{\alpha_1,\alpha_2}((Ly)_{j,k},\alpha_1,\alpha_2)) + \text{E}(M_{\alpha_1,\alpha_2}((Ly)_{j,k},\alpha_1,\alpha_2)) \quad (17)$$

where

$$\text{Mean}_{\alpha_1,\alpha_2}((L\beta)_{j,k}) = \int_{\alpha_1}^{\alpha_2}\sqrt{\frac{|\alpha_1-\alpha_2|}{2\pi^2\sigma^2}}(L\beta)_{j,k}\exp\left\{-|\alpha_1-\alpha_2|\,||(Ly)_{j,k}||_2^2\right\} \times \exp\left\{\frac{-||(Ly)_{j,k}-(L\beta)_{j,k}||_2^2}{2\sigma^2}\right\}d(Ly)_{j,k} + \int_{\alpha_2}^{\infty}\frac{(L\beta)_{j,k}}{\sqrt{2\pi\sigma^2}}\exp\left\{\frac{-||(Ly)_{j,k}-(L\beta)_{j,k}||_2^2}{2\sigma^2}\right\}d(Ly)_{j,k}, \quad (18)$$

and

$$\text{E}_{\alpha_1,\alpha_2}((L\beta)_{j,k})^2 = \int_{\alpha_1}^{\alpha_2}\sqrt{\frac{|\alpha_1-\alpha_2|}{2\pi^2\sigma^2}}(L\beta)_{j,k}^2\exp\left\{-2|\alpha_1-\alpha_2|\,||(Ly)_{j,k}||_2^2\right\} \times \exp\left\{\frac{-||(Ly)_{j,k}-(L\beta)_{j,k}||_2^2}{2\sigma^2}\right\}d(Ly)_{j,k} + \int_{\alpha_2}^{\infty}\frac{(L\beta)_{j,k}^2}{\sqrt{2\pi\sigma^2}}\exp\left\{\frac{-||(Ly)_{j,k}-(L\beta)_{j,k}||_2^2}{2\sigma^2}\right\}d(Ly)_{j,k}, \quad (19)$$

then the varaince and the risk can be computed form the equations (17) and (18).

4 Control the parameters α_1 and α_2

The biggest challenge is to specify the values of thresholding α_1 and α_2. The popular choice for choosing the value of the parameter α_1 is the universal threshold, is defined as

$$\alpha_1 = \hat{\sigma}\sqrt{2\log_2(n)}, \quad (20)$$

where $\hat{\sigma}$ is estimated the noise level for high resolution of wavelet coefficients as $\hat{\sigma} = \text{Median}((Ly)_{J-1,.})$, and n is the number of wave points–see [13] and [11] for more details. The parameter α_2 in the new proposed thresholding rule can be computed by

$$\alpha_2 = 2\alpha_1, \quad (21)$$

this method was suggest by [20] where it was successfully used in spectral density estimation. In this article, the minimum mean square error is apply to use the results as fix point. The mean idea of the minimum mean square error is to find the value of the threshold which makes the L_2 small. Moreover, the producer of minimum mean square error can be explained as

1. Propose the value of threshold and then used to compute the thresholding rule.
2. Compute the Mean square error.
3. Repeat the step one and two.
4. Compute the average of MSE.

The average of the mean square error can be computed by the following form

$$AMSE(\beta) = \frac{1}{kn}\sum_{j=1}^{k}\sum_{i=1}^{n}(\beta_i-\hat{\beta}_i)_j^2, \quad (22)$$

where n is the number of wave points and k is the number of replication, this can be used for the model 1 and the model 2.

Table 1: The results of AMSE for the Hard, Soft and the new proposed thresholding rules to estimate the Doppler signal with different levels of noise and blur. The red lines shows minimum AMSE result at each row.

n	γ	σ	Method	AMSE	Method	AMSE	Method	AMSE
32	0.01	0.1	H_α	1.610119	S_α	1.610124	M_{α_1,α_2}	1.610070
		0.2		1.832931		1.798107		1.814126
		0.3		1.937834		1.990426		1.931449
		0.5		1.856546		2.012618		1.929785
	0.02	0.1		3.057686		2.992644		3.122664
		0.2		3.535243		3.751970		3.535094
		0.3		3.691593		3.843839		3.759440
		0.5		3.354209		3.187035		3.392629
	0.03	0.1		5.219001		5.218854		5.219250
		0.2		5.221337		5.220493		5.220336
		0.3		5.005338		5.086855		5.129062
		0.5		4.214870		4.146241		4.250563
	0.05	0.1		5.620662		5.619543		5.619304
		0.2		5.594430		5.628892		5.629080
		0.3		5.208057		5.111638		5.046385
		0.5		5.530406		5.326494		5.369827
64	0.01	0.1	H_α	0.0008044755	S_α	0.01272352	M_{α_1,α_2}	0.01255887
		0.2		0.0085782356		0.08438633		0.08427372
		0.3		0.0425867517		0.27448985		0.27505246
		0.5		0.3515195470		1.14283750		1.13602783
	0.02	0.1		0.006094985		0.04490323		0.04299602
		0.2		0.048819972		0.32882920		0.33698606
		0.3		0.351650287		1.05202431		1.15375488
		0.5		2.188631875		3.28372721		3.27003979
	0.03	0.1		0.02223674		0.1192502		0.1257178
		0.2		0.32299826		0.9184411		0.8891355
		0.3		1.23417318		2.4897441		2.5414767
		0.5		4.46438068		4.7384630		4.8008343
	0.05	0.1		0.07956636		0.4441768		0.440935
		0.2		1.63625337		2.7591055		2.721683
		0.3		4.36172995		4.7381470		4.623866
		0.5		10.54483710		7.6615978		7.765297
128	0.01	0.1	H_α	0.001605696	S_α	0.01248386	M_{α_1,α_2}	0.003433704
		0.2		0.029166190		0.12644387		0.031575849
		0.3		0.121893613		0.41438411		0.160883521
		0.5		0.916280747		1.63841578		1.917945590
	0.02	0.1		0.02898089		0.1119685		0.08056947
		0.2		0.35323938		0.7780431		0.40749165
		0.3		1.44976184		1.8476726		1.39150223
		0.5		3.83819638		3.8464096		5.30061382
	0.03	0.1		0.1143283		0.3739481		0.3921199
		0.2		1.4130167		1.8608519		1.6074033
		0.3		3.1698182		3.1317615		3.2525353
		0.5		10.1434473		6.2523934		7.1991858
	0.05	0.1		0.6001335		1.264580		2.486832
		0.2		3.6497703		3.510369		4.445732
		0.3		10.0125309		6.097469		8.851026
		0.5		22.9699236		10.004043		15.205268

5 Simulation

Simulation study is applied using a wave which is intrduced by [11]. Hence the the code starts from level $j_0 = 3$, as suggested by [12]. The wave can be chosen for different equally spaced points $n = \{32, 64, 128\}$, it corrupted by different levels of matrix transformation by taking in the true wave $\gamma = \{0.01, 0.02, 0.03, 0.05\}$ in (3) and the wave corrupted by level of noise, independent Gaussian noise with zero mean and standard deviation $\sigma = \{0.1, 0.2, 0.3, 0.5\}$ in models (1) and (2). For the second model the form of the estimation is used and it takes the form

$$\hat{\beta} = (Z^T Z)^{-1} Z^T T_\alpha(y), \tag{23}$$

where Z is the transformation matrix in (3) and T is one for the thresholding rule which is Hard, Soft, or the new proposed rule. Hence, the estimation in (23) can be explained as the first regression process, and then thresholding method. Table 1 shows the results of different rules, the Hard thresholding in 10 provides a good estimate for the Doppler signal. Hence, as the number of points increase the MSE becomes small, because the observation have information about the underlying wave.

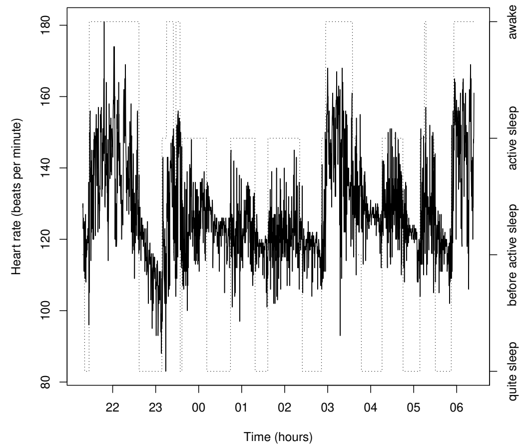

Fig. 5: Plots of BabyECG data (solid line) and sleep state (dashed line), the number of observations is 2048, equally spaced points.

6 Application to medical data

The Hard, Soft and the suggested method are applied to a real data, which is inductance plethysmography data to estimate an underlying wave. The data collected by the Department of Anaesthesia at the Bristol Royal Infirmary. The number of observations is 2048, equally spaced points, with variance equals 190.8263, Median equals 125.0 and Mean equals 127.6. anthers can access the data within WaveThresh using the code $data(BabyECG)$. Moreover, the structure of the sleep state can be downloaded using $data(BabySS)$. Figure 5 shows the plots of BabyECG and sleep stateduring the time (21 PM-7 AM). Hence, the aim of the investigation of the BabyECG was to specify the sleep state successfully from the observations by removing the noise and blur. These data were studied and investigated by other authors, for example, [21], [22] and [23]. Now, the proposed method, Hard and soft applied to the real data. Figure 6 shows the plots of different thresholding rules; Hard rules gives the estimation of the data, however, the noise still appeared in Figure 6(a). Soft thresholding provides better estimation than Hard, however, the noise still appeared in Figure 6(b). The proposed method gives a good result comparing with Hard and soft rules.

7 Conclusion

In this article, Doppler wave was studying using wavelet basis and a new thresholding method is considered to

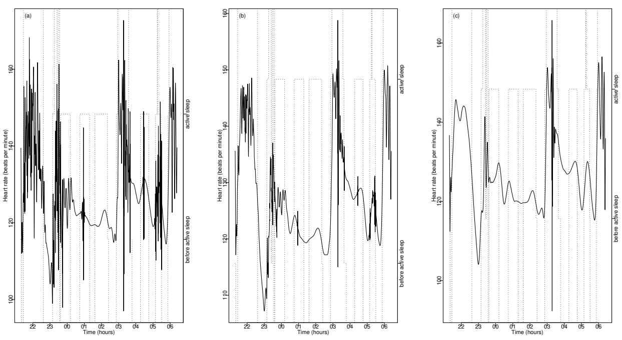

Fig. 6: Plots of the result of different thresholding rules; Hard (a), Soft (b), and the proposed method (c) for BabyECG data.

remove the noise and the blur by using the normal transformation matrix. The proposed method was compared to state-of-the-art methods. Moreover, Hard and Soft thresholding rules were applied to the Doppler wave, providing a good results. However, the proposed method gives a good result as applying to the real data. Finally, the normal transformation matrix was applied to the real data for removing the blur, however, the results are not acceptable.

References

[1] J. Morlet, Issues in acoustic Signal—image processing and recognition, Sampling theory and wave propagation, 233–261, (1983).

[2] R. Kronland-Martinet, J. Morlet, and A. Grossmann, Analysis of sound patterns through wavelet transforms, International journal of pattern recognition and artificial intelligence,**1**, (2), 273–302, (1987).

[3] S. G. Mallat, A theory for multiresolution signal decomposition: the wavelet representation, IEEE transactions on pattern analysis and machine intelligence, **1**1, (7), 674–693, (1989).

[4] G. Beylkin, and R. Coifman and V. Rokhlin, Fast wavelet transforms and numerical algorithms I, Communications on pure and applied mathematics, **4**4, (2), 141–183, (1991).

[5] J. M. Reid and M. P. Spencer, Ultrasonic Doppler technique for imaging blood vessels, Science, **1**76, (4040), 1235–1236, (1972).

[6] R. Aaslid, T. Markwalder and H. Nornes, Noninvasive transcranial Doppler ultrasound recording of flow velocity in basal cerebral arteries, Journal of neurosurgery, **5**7, (6), 769–774, (1982).

[7] L. Hatle, Doppler ultrasound in cardiology, Physical Principles and Clinical Applications, 77–89, (1982).

[8] S. J. Goldberg, H. D. Allen, G. R. Marx and R. L. Donnerstein, Doppler echocardiography, (1988).

[9] O. J. Ginther, Ultrasonic imaging and animal reproduction, (No Title), (1995).

[10] P. Sladkevicius, L. Valentin and K. Maršál, Blood flow velocity in the uterine and ovarian arteries during the normal menstrual cycle, Ultrasound in Obstetrics and Gynecology: The Official Journal of the International Society of Ultrasound in Obstetrics and Gynecology, **3**, (3), 199–208, (1993).

[11] D. L. Donoho and L. M. Johnstone, Ideal spatial adaptation by wavelet shrinkage, biometrika, **8**1, (3), 425–455, (1994).

[12] A. Antoniadis, J. Bigot and T. Sapatinas, Wavelet estimators in nonparametric regression: a comparative simulation study, Journal of statistical software, **6**, 1–83,(2001).

[13] G. P. Nason, Wavelet methods in statistics with R, New York: Springer, (2008).

[14] B. Vidakovic, Statistical modeling by wavelets, united state: John Wiley & Sons, (2009).

[15] R. Sobolu and D. Pusta, Wavelet Methods in Nonparametric Regression Based on Experimental Data, Bulletin UASVM Horticulture, **6**6, (2),(2009).

[16] M. J. Jensen, Ordinary least squares estimate of the fractional differencing parameter using wavelets as derived from smoothing kernels, Southern Illinois University, Carbondale, (1995).

[17] S. Barber and G. P. Nason, Real nonparametric regression using complex wavelets, Journal of the Royal Statistical Society Series B: Statistical Methodology, **6**6, (4), 927–939, (2004).

[18] G. P. Nason, Choice of the threshold parameter in wavelet function estimation, Wavelets and statistics, 261–280, (1995).

[19] M. Raimondo, Wavelet shrinkage via peaks over threshold, InterStat, 1–19, (2002).

[20] A. T. Walden, Andrew T, D. B. Percival and E. J. McCoy, Spectrum estimation by wavelet thresholding of multitaper estimators, IEEE Transactions on Signal Processing, **4**6, (12), 3153–3165, (1998).

[21] G. P. Nason, Wavelet shrinkage using cross-validation, Journal of the Royal Statistical Society. Series B (Methodological), 463–479, (1996).

[22] F. Abramovich and B. W. Silverman, Wavelet decomposition approaches to statistical inverse problems, Biometrika, **8**5, (1), 115–129, (1998).

[23] F. Abramovich, P. Besbeas, and T. Sapatinas, Empirical Bayes approach to block wavelet function estimation, Computational Statistics and Data Analysis, **3**9, (4), 435–451, (2002).

Maha M. Helmi received the PhD degree in Applied Mathematics at Keele university . Her research interests are in the areas of applied mathematics and Continuum mechanics including the deformation and transmission materials, material engineering, mathematical physics, wave propagation in elastic media. She has published research articles in international journals of mathematical and engineering sciences